

# Overcome uncertainties of vertical take-off and landing aircraft based on optimal sliding mode control

Wajdi Sadik About<sup>1</sup>, Hayder S. Abd Al-Amir<sup>2</sup>, Aseel A. Alhamdany<sup>3</sup>, Fahad M. Kadhim<sup>1</sup>

<sup>1</sup>Department of Prosthetics and Orthotics Engineering, College of Engineering, Al-Nahrain University, Baghdad, Iraq

<sup>2</sup>Department of Power Mechanics, Institute of Technology, Middle Technical University, Baghdad, Iraq

<sup>3</sup>Department of Electromechanical Engineering, University of Technology, Baghdad, Iraq

## Article Info

### Article history:

Received Aug 7, 2022

Revised Oct 11, 2022

Accepted Oct 24, 2022

### Keywords:

Particle swarm optimization

Sliding mode control

Stability

Tracking

Vertical take-off and landing aircraft

Vibration

## ABSTRACT

This study aims to design a robust and optimal controller to overcome the problems related to the existence of disturbances and uncertainties during takeoff and landing operations of vertical take-off and landing (VTOL) aircraft. The dynamics are decomposed into two phase's parts which are the minimum phase and the non-minimum phase. These two-part are controlled by proposing a robust nonlinear controller represented by sliding mode control (SMC). Also, the chattering effect due to the fast-switching surface in SMC is eliminated by utilizing a proposed sigmoid function which acts as the sigmoid function. The controller's main parameters are tuned optimally based on the particle swarm optimization (PSO) algorithm. In addition, the controller guaranteed the system stability based on the Lyapunov and Routh theories. The main output parameter responses represented by the positioning of the centre of mass and angle of rolling are determined with bounded control inputs. The performance of the proposed controller is tested by tracking VTOL parameters to the desired trajectories. The simulated results not only showed a significant tracking trajectory but also system stability guaranteed. In addition, the results showed an improved rate of 72% and 84% compared with those results obtained from the literature.

*This is an open access article under the [CC BY-SA](https://creativecommons.org/licenses/by-sa/4.0/) license.*



## Corresponding Author:

Wajdi Sadik About

Department of Prosthetics and Orthotics Engineering, College of Engineering, Al-Nahrain University

Baghdad, Iraq

Email: wajdisadik@gmail.com

## 1. INTRODUCTION

Fixed-wing combat aircraft is considered one of the most important tools of modern armies because of their combat, defence, and reconnaissance missions. The main important requirement for this type of aircraft is large and flat areas for take-off and landing. These areas are known as airports, whether they are on land or on ships. These airports are far from the battlefield and cannot always be provided near them. Therefore, there was a need to think about adding the vertical take-off and landing (VTOL) feature to fixed-wing aircraft as in helicopters. That supports these types of aircraft to land almost anywhere and eliminates the need for long airport runways. This helps to reduce the risks associated with the movement of the aircraft when taking off and landing, especially on battlefronts. The VTOL aircraft have many applications and usages such as reconnaissance, search and rescue, logistics and other fields. The most important feature is the use of secret places that can be hidden for take-off and landing. The landing gear of this type of aircraft is less complicated than that of fixed-wing aircraft. However, it needs flat land without ripples to land and takes off, which reduces its work in all types of terrain and limits its capabilities. It is noteworthy that there are numerous types of VTOL vehicles, which it was listed through a reference [1]. The most worrying of the

engineering designers is the necessity of having high stability of the plane for vertical take-off and landing. This is represented by preventing rotations around its own three axes (yaw-roll-pitch), especially in difficult weather conditions such as high wind. During the take-off and landing of VTOL aircraft, due to the presence of a vertical thrust downward, uneven forces appear on both ends of the wing in the vertical direction, which causes a roll moment reaction about the aircraft's longitudinal axis. The slight lateral acceleration of the aircraft will be generated as presented in the current interesting study. This phenomenon makes the plane unstable. The problem of the stability of the aircraft at vertical take-off and landing has been solved by introducing the error tracking system that occurs with the stability of the aircraft in the horizontal plane.

To study the stability of the aircraft during take-off and landing, simplified two-dimensional mathematical models have been developed that simulate well the dynamic behaviour of the aircraft. These mathematical models have proven their efficiency and quality for various scientific applications over the past years. Then provide the available automated control algorithms for the desired results. Real experiments on control equipment are very expensive in terms of manufacturing technology as well as in terms of testing stages or trials. The presence of these models allows researchers to develop models of control units of various types to simulate the control of aircraft movement during take-off and landing and increase its stability [2]-[4]. These controller structures were built on one tracking control algorithm such as approximation input-output linearization [5], system inversion [6], linear optimal control [7], internal-model based approach [8], backstepping [9], and Lyapunov function technique [10]. To achieve the reality of dynamic systems, (certainty) coefficients are introduced to examine and develop the proposed controls to be more realistic before they are applied to the systems in real life. Researchers have introduced many control strategies during the take-off and landing of aircraft (VTOL), to make them more stable and safe under various conditions. The controller type proportional, integral and derivative (PID) has been used a lot with linear models because it is still really simple and easy to control and implement later as in [11]-[15]. Waslander *et al.* [16], a comparison of two nonlinear controllers based on integral sliding mode and reinforcement learning is presented. More recently, the studies focused on robust controllers when disturbances and uncertainties were available [17]-[21]. All control systems applied in the field of aircraft seek to make the angle of rolling close to zero and reduce the hover fluctuation of the aircraft during vertical take-off and landing as well as suppression of the undesired vibrations. Generally, there is a lot of work that has to be done using the available control theories to practical implementation and down to complex details.

The essential motivation of this study is possessed from [16], [17], [20] because the stabilization issue of the VTOL at the centre of mass for the aircraft is still there waiting to be treated. This can be done by producing force control actions for the VTOL able to track the desired trajectories with a minimum error. And also able to eliminate unwanted bounded disturbances. Moreover, the characterization of the contribution of this research according to the comparisons with the literature that includes different types of nonlinear controllers for VTOL can be enumerated as follows: i) the control law for both the minimum phase and the non-minimum phase dynamic parts is developed based on very accurate analytical derivation using sliding mode control (SMC). In addition, the stability based on Lyapunov and Routh criteria is guaranteed and ensures optimal control forces for fast control action by using the particle swarm optimization algorithm technique; ii) very fast tracking trajectory and minimum tracking error for different initial states; iii) the chattering phenomena of the sliding mode control are eliminated by minimizing the output of the signum function with the minimum value as possible; and iv) the proposed controller is capable to overcome the effects of undesirable disturbances and parameters uncertainties effectively.

In this study, the dynamic mathematical model of the VTOL based on Newton's law is derived and analysed. The derived dynamic decomposed into the minimum phase dynamic part and the non-minimum phase dynamic part. The first part is used to control the vertical dynamic of the flight and the latter part is used to control both the horizontal and roll dynamic of the flight. Optimal SMC with bounded input control is proposed to obtain trajectory tracking and stability. This work aims to provide a tracking automatic control with a high potential to control the movement of the aircraft during vertical take-off and landing. This was achieved by making the angle of rolling close to zero and reducing the hover fluctuation of the aircraft during vertical take-off and landing as well as suppressing the undesired vibrations.

## 2. MATHEMATICAL MODEL OF VTOL

According to Figure 1 and based on the principles of Newton's law, and let the small coefficient,  $\varepsilon_0$ , which describes the relationship between the lateral force,  $\varepsilon_0 l$ , and the rolling moment of the VTOL aircraft, the dynamic model is derived as [5], [6]:

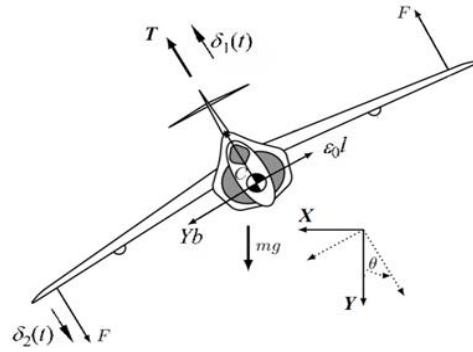


Figure 1. Planar VTOL aircraft

$$\begin{aligned}
 -m\ddot{X} &= -(T + \delta_1(t))\sin(\theta) + \varepsilon_0(l + \delta_2(t))\cos(\theta) \\
 -m\ddot{Y} &= -(T + \delta_1(t))\cos(\theta) + \varepsilon_0(l + \delta_2(t))\sin(\theta) - mg \\
 I_z\ddot{\theta} &= l + \delta_2(t)
 \end{aligned}
 \tag{1}$$

The dynamic model given in (1) can be rescaled with the following are define  $x = -X/g$ ,  $y = -Y/g$ ,  $u_1 = T/(mg)$ ,  $u_2 = l/I_z$ ,  $\varepsilon = \varepsilon_0 I_z / (mg)$ ,  $\xi_1(t) = \delta_1(t)/(mg)$ ,  $\xi_2(t) = \delta_2(t)/I_z$ . Then, the dynamic model can be written as (2).

$$\begin{aligned}
 \ddot{x} &= -(u_1 + \xi_1(t))\sin(\theta) + \varepsilon(u_2 + \xi_2(t))\cos(\theta) \\
 \ddot{y} &= -(u_1 + \xi_1(t))\cos(\theta) + \varepsilon(u_2 + \xi_2(t))\sin(\theta) - g \\
 \ddot{\theta} &= u_2 + \xi_2(t)
 \end{aligned}
 \tag{2}$$

Suppose that  $x_1 = x$ ,  $x_2 = \dot{x}$ ,  $y_1 = y$ ,  $y_2 = \dot{y}$ . Then, the scaled mathematical dynamic equation of VTOL becomes as below;

$$\begin{aligned}
 \dot{x}_1 &= x_2 \\
 \dot{x}_2 &= -(u_1 + \xi_1(t))\sin(\theta) + \varepsilon(u_2 + \xi_2(t))\cos(\theta) \\
 \dot{y}_1 &= y_2 \\
 \dot{y}_2 &= (u_1 + \xi_1(t))\cos(\theta) + \varepsilon(u_2 + \xi_2(t))\sin(\theta) - g \\
 \dot{\theta} &= \omega \\
 \dot{\omega} &= u_2 + \xi_2(t)
 \end{aligned}
 \tag{3}$$

where  $x_1(t)$  and  $y_1(t)$  are represent the positioning of the centre of mass for the aircraft,  $\theta(t)$  is the angle of rolling,  $x_2(t)$  and  $y_2(t)$  are represent the linear and angular velocities respectively, the  $\varepsilon$  is defined as the constant of coupling between the lateral force and the rolling moment and  $g$  is the gravitation acceleration. The control inputs,  $u_1$  and  $u_2$ , represent the thrust and rotational moment respectively. The uncertainties of the systems are defined by  $\delta_1$ ,  $\delta_2$ , and  $\delta_3$ . It is clear from the model given in (1) that the aircraft model is not only underactuated but also in a non-minimum phase when  $\varepsilon \neq 0$  concerning the nominal output  $y$ . Consider,

$$\begin{aligned}
 d_1(t) = \delta_1(t) &= -\xi_1(t)\sin\theta + \varepsilon \xi_2\cos\theta \\
 d_2(t) = \delta_2(t) &= \xi_1(t)\cos\theta + \varepsilon \sin\theta \\
 d_3(t) = \delta_3(t) &= \xi_2
 \end{aligned}
 \tag{4}$$

in this study, the differences between outputs of the VTOL system and the assumed desired trajectory,  $(x_d, y_d)$ , can be defined as the tracking error:

$$\begin{aligned}
 \dot{e}_1 &= e_2 \\
 \dot{e}_2 &= -(u_1 + \xi_1(t))\sin(\theta) + \varepsilon(u_2 + \xi_2(t))\cos(\theta) - \dot{x}_d \\
 \dot{e}_3 &= e_4 \\
 \dot{e}_4 &= -(u_1 + \xi_1(t))\cos(\theta) + \varepsilon(u_2 + \xi_2(t))\sin(\theta) - g - \dot{y}_d \\
 \dot{\theta} &= \omega \\
 \dot{\omega} &= u_2 + \xi_2(t)
 \end{aligned}
 \tag{5}$$

from (5), the following expression can be driven [5].

$$\begin{bmatrix} \dot{e}_2 \\ \dot{e}_4 \end{bmatrix} = \begin{bmatrix} -\sin\theta & \varepsilon\cos\theta \\ \cos\theta & \varepsilon\sin\theta \end{bmatrix} \begin{bmatrix} u_1 \\ u_2 \end{bmatrix} + \begin{bmatrix} \xi_1\sin\theta + \varepsilon\xi_2\sin\theta \\ \xi_1\cos\theta + \varepsilon\xi_2\cos\theta \end{bmatrix} + \begin{bmatrix} -\ddot{x}_d \\ -g - \dot{y}_d \end{bmatrix} \quad (6)$$

The utilizing of the input state linearization is necessary because the relative degree for the vector of (5) corresponding to the output is [2 2]. This is can be done by adopting the control law presented in [22], [23]. So,

$$\begin{bmatrix} u_1 \\ u_2 \end{bmatrix} = \begin{bmatrix} -\sin\theta & \varepsilon\cos\theta \\ \cos\theta & \varepsilon\sin\theta \end{bmatrix}^{-1} \begin{bmatrix} \lambda_1 + \ddot{x}_d \\ \lambda_2 + g + \dot{y}_d \end{bmatrix} \quad (7)$$

by the following steps, the  $\lambda_1$  and  $\lambda_2$  can be designed [5].

$$\begin{bmatrix} -\sin\theta & \varepsilon\cos\theta \\ \cos\theta & \varepsilon\sin\theta \end{bmatrix}^{-1} = \begin{bmatrix} -\sin\theta & \cos\theta \\ \frac{1}{\varepsilon}\cos\theta & \frac{1}{\varepsilon}\sin\theta \end{bmatrix} \quad (8)$$

Therefore, converts (5) to,

$$\begin{aligned} \dot{e}_1 &= e_2 \\ \dot{e}_2 &= \lambda_1 + \delta_1(t) \\ \dot{e}_3 &= e_4 \\ \dot{e}_4 &= \lambda_2 + \delta_2(t) \\ \dot{\theta} &= \omega \\ \dot{\omega} &= u_2 + \delta_3(t) \end{aligned} \quad (9)$$

then the following formula can be drawn from (7) and (8);  $u_2 = \frac{1}{\varepsilon} \lambda_1 \cos\theta + \frac{1}{\varepsilon} \lambda_2 \sin\theta + \frac{g}{\varepsilon} \sin\theta + \frac{1}{\varepsilon} \ddot{x}_d \cos\theta + \frac{1}{\varepsilon} \dot{y}_d \sin\theta$ . Based on that, the following equation is provided;

$$\begin{aligned} \dot{e}_1 &= e_2 \\ \dot{e}_2 &= \lambda_1 + \delta_1(t) \\ \dot{e}_3 &= e_4 \\ \dot{e}_4 &= \lambda_2 + \delta_2(t) \\ \dot{\theta} &= \omega \\ \dot{\omega} &= \frac{1}{\varepsilon} \lambda_1 \cos\theta + \frac{1}{\varepsilon} \lambda_2 \sin\theta + \frac{g}{\varepsilon} \sin\theta + \frac{1}{\varepsilon} \ddot{x}_d \cos\theta + \frac{1}{\varepsilon} \dot{y}_d \sin\theta + \xi_2(t) \end{aligned} \quad (10)$$

a new variable,  $\chi$ , instead of  $\omega$  is considered for eliminating  $\lambda_1$  and  $\lambda_2$  in  $\dot{\omega}$  as (11) [22], [23].

$$\chi = \varepsilon\omega - e_2\cos\theta - e_4\sin\theta \quad (11)$$

From (11), it can be seen that if  $e_2 \rightarrow 0$ ,  $e_4 \rightarrow 0$ , then  $\chi \rightarrow \varepsilon\omega$ , and if  $\chi \rightarrow 0$ , then  $\omega \rightarrow 0$ , so that  $\chi$  can be used instead of  $\omega$  [22], [23]. Also, it can be seen that  $\dot{\omega}$  includes  $\lambda_1$  and  $\lambda_2$ ,  $\dot{e}_2$  includes  $\lambda_1$ , and  $\dot{e}_4$  includes  $\lambda_2$ , so by combining  $\omega$ ,  $\chi$ ,  $e_4$  the  $\chi$  could be designed. Thus, the differential equation  $\dot{\chi}$  can get with  $\dot{\omega}$ ,  $\dot{e}_2$ , and  $\dot{e}_4$ . Therefore, the elimination of  $\lambda_1$ ,  $\lambda_2$  is possible [22]. So, from (11), one can get (12).

$$\omega = \dot{\theta} = \frac{1}{\varepsilon}(\chi + e_2\cos\theta - e_4\sin\theta) \quad (12)$$

Then,

$$\begin{aligned} \dot{\chi} &= \varepsilon\dot{\omega} - \dot{e}_2\cos\theta + e_4\dot{\theta}\sin\theta - \dot{e}_4\sin\theta - e_4\dot{\theta}\cos\theta \\ &= \varepsilon\left(\frac{1}{\varepsilon}\lambda_1\cos\theta + \frac{1}{\varepsilon}\lambda_2\sin\theta + \frac{g}{\varepsilon}\sin\theta + \frac{1}{\varepsilon}\ddot{x}_d\cos\theta + \frac{1}{\varepsilon}\dot{y}_d\sin\theta + \xi_2(t)\right) \\ &\quad - (\lambda_1 - \xi_1(t)\sin\theta + \varepsilon\xi_2(t)\cos\theta)\cos\theta - (\lambda_2 + \xi_1(t)\cos\theta \\ &\quad + \varepsilon\xi_2(t)\sin\theta)\sin\theta + \frac{1}{\varepsilon}(e_2\sin\theta - e_4\cos\theta)(\chi + e_2\cos\theta + e_4\sin\theta) \\ &= \frac{1}{\varepsilon}(e_2\sin\theta - e_4\cos\theta)(\chi + e_2\cos\theta + e_4\sin\theta) + g\sin\theta + \ddot{x}_d\cos\theta + \dot{y}_d\sin\theta \end{aligned} \quad (13)$$

hence, the dynamics part of the non-minimum phase is obtained from (12) as (14).

$$\dot{\bar{\chi}} = q(e_1, e_2, e_3, e_4, \theta, \chi, Y_d) \tag{14}$$

where  $\bar{\chi} = [\theta \ \chi]^T$ ,  $Y_d = [\ddot{x}_d \ \ddot{y}_d]$ , and,

$$q(e_1, e_2, e_3, e_4, \theta, \chi, Y_d) = \begin{bmatrix} \frac{1}{\varepsilon}(\chi + e_2 \cos\theta + e_4 \sin\theta) \\ \frac{1}{\varepsilon}(e_2 \sin\theta - e_4 \cos\theta)(\chi + e_2 \cos\theta + e_4 \sin\theta) + g \sin\theta + \ddot{x}_d \cos\theta + \ddot{y}_d \sin\theta \end{bmatrix}$$

It is evident from the latter equations that the  $q(\cdot)$  is related to  $[e_1 \ e_2]$  at zero states but it does not to  $[e_3 \ e_4]$ . Therefore, the following can be derived [22], [23].

$$\left. \frac{\partial q(e_1, e_2, e_3, e_4, \theta, \chi, Y_d)}{\partial(e_3 \ e_4)} \right|_{\Pi} = \Pi_{2 \times 2} \tag{15}$$

$$\left. \frac{\partial q(e_1, e_2, e_3, e_4, \theta, \chi, Y_d)}{\partial(e_1 \ e_2)} \right|_{\Pi} \neq \Pi_{2 \times 2} \tag{16}$$

Based on (15) and (16), it is clear that the model given in (10) can be decomposed into two parts. The first one is the minimum phase part that is associated with control of vertical flight dynamics and the second one is the non-minimum phase part that is associated with control of the coupled horizontal and roll flight dynamics. The two parts models are presented in (17) and (18) respectively.

$$\begin{aligned} \dot{e}_3 &= e_4(t) \\ \dot{e}_4 &= \lambda_2 + \delta_2(t) \end{aligned} \tag{17}$$

$$\begin{aligned} \dot{e}_1 &= e_2 \\ \dot{e}_2 &= \lambda_1 + \delta_1(t) \\ \dot{\theta} &= \frac{1}{\varepsilon}(\chi + e_2 \cos\theta - e_4 \sin\theta) \\ \dot{\chi} &= \frac{1}{\varepsilon}(e_2 \sin\theta - e_4 \cos\theta)(\chi + e_2 \cos\theta + e_4 \sin\theta) + (g + \ddot{y}_d) \sin\theta + \ddot{x}_d \cos\theta \end{aligned} \tag{18}$$

### 3. THE DESIGN OF THE OPTIMAL CONTROLLER

This study uses feedback inversion represented by a conventional sliding mode controller to resolve the output-tracking problem for the minimum phase dynamics given by (17). The SMC is selected as (19):

$$\sigma_1 = ce_3 + \dot{e}_3, \quad e_3(t) = y_1 - y_d, \quad e_4(t) = y_2 - \dot{y}_d \tag{19}$$

where  $c$  is a positive scalar parameter used to guarantee the system trajectory to hit the sliding surface when  $t \rightarrow \infty$ , i.e.  $c > 0$ , then the controller is selected:

$$\lambda_2 = -ce_4 - \bar{h}_1 \text{sgn}(\sigma_1) \tag{20}$$

where  $\bar{h}_1 \geq |d_2(t)|$ , and  $\text{sgn}$  is the signum function that is proposed in this study as a sigmoid function,  $\text{sgn}(\sigma_i) = c \tanh(\sigma_i)$  where  $i = 1, 2$ , to reduce or overcome the chattering effect related to the SMC [24].

The Lyapunov function is defined as  $V_1 = \frac{1}{2}\sigma_1^2$ , then the following can be derived [25], [26].

$$\begin{aligned} \dot{V}_1 &= \sigma_1 \dot{\sigma}_1 = (c\dot{e}_3 + \dot{e}_4) = \sigma_1 (ce_4 + (\lambda_2 + d_2)) = \sigma_1 (ce_4 + (-ce_4 - \bar{h}_1 \text{sgn}(\sigma_1) + d_2)) \\ &= \sigma_1 (-\bar{h}_1 \text{sgn}(\sigma_1) + d_2) = c(-\bar{h}_1 |\sigma_1| + d_2 \sigma_1) \leq 0 \end{aligned} \tag{21}$$

Therefore, for any differential output command  $y_d$ ,  $y_1(t) \rightarrow y_d$ ,  $y_2(t) \rightarrow \dot{y}_d$  as  $t \rightarrow \infty$ . Thus the vertical dynamics and both the horizontal and roll dynamics of the aircraft do not affect each other because the minimum phase dynamics and the non-minimum phase dynamics are completely decoupled. Here, the main goal is to design SMC using the above sigmoid function to stabilize the system regarding the non-minimum phase dynamics. So, for (18), let denote,

$$\mu_1 = e_2, \mu_2 = [e_1 \ \theta \ \chi]^T, e_1 = x_1 - x_d, e_2 = x_2 - \dot{x}_d \tag{22}$$

then, (18) is written as;

$$\begin{aligned} \dot{\mu}_1 &= \lambda_1 + d_1(t) \\ \dot{\mu}_2 &= p(e_1, e_2, e_3, e_4, \theta, \chi, Y_d) \end{aligned} \tag{23}$$

where  $p(e_1, e_2, e_3, e_4, \theta, \chi, Y_d) = \begin{bmatrix} e_2 \\ \frac{1}{\varepsilon}(\chi + e_2 \cos \theta + e_4 \sin \theta) \\ \frac{1}{\varepsilon}(\chi + e_2 \cos \theta + e_4 \sin \theta)(e_2 \sin \theta - e_4 \cos \theta + \ddot{x}_d \cos \theta + (\ddot{y}_d + g) \sin \theta) \end{bmatrix}$

based on Taylor's expansion, (23) can be written as,

$$\begin{aligned} \dot{\mu}_2 &= \frac{\partial p}{\partial e_2} \Big|_{\Pi} e_2 + \frac{\partial p}{\partial [e_1 \ \theta \ \chi_2]} \Big|_{\Pi} [e_1 \ \theta \ \chi_2]^T + \Pi(e_1, e_2, e_3, e_4, \theta, \chi, Y_d) \\ &= \tilde{A}_{21} \mu_1 + \tilde{A}_{22} \mu_2 + \Pi(e_1, e_2, e_3, e_4, \theta, \chi, Y_d) \end{aligned} \tag{24}$$

where,

$$\tilde{A}_{21} = \frac{\partial p(e_1, e_2, e_3, e_4, \theta, \chi, Y_d)}{\partial e_2} \Big|_{\Pi} = [1 \ \varepsilon^{-1} \ \Pi]^T, \quad \tilde{A}_{22} = \frac{\partial p(e_1, e_2, e_3, e_4, \theta, \chi, Y_d)}{\partial (e_1 \ \theta \ \chi_2)} \Big|_{\Pi} = \begin{bmatrix} 0 & 0 & 0 \\ 0 & 0 & \varepsilon^{-1} \\ 0 & g & 0 \end{bmatrix}$$

$$\Pi(e_1, e_2, e_3, e_4, \theta, \chi, Y_d) = p(e_1, e_2, e_3, e_4, \theta, \chi, Y_d) - \tilde{A}_{22} \mu_2 - \tilde{A}_{21} \mu_1$$

The sliding variable for (23) is defined as,

$$\sigma_2 = \mu_1 - \mathbf{M} \mu_2 \tag{25}$$

where  $\mathbf{M} = [m_1 \ m_2 \ m_3]$  and  $\mathbf{M}$  is selected in such a way that let  $\tilde{A}_{22} + \tilde{A}_{21} \mathbf{M}$  Hurwitz. According to (25), the sliding time,  $t_s$ , exists if and only if the sliding mode exists. Therefore, for  $t \geq t_s$  which let  $\sigma_2 = 0$ , then the following can be derived based on (24).

$$\begin{aligned} \dot{\mu}_2 &= \tilde{A}_{21} \mathbf{M} \mu_2 + \tilde{A}_{22} \mu_2 + \Pi(e_1, e_2, e_3, e_4, \theta, \chi, Y_d) \\ &= (\tilde{A}_{21} \mathbf{M} + \tilde{A}_{22}) \mu_2 + \Pi(e_1, e_2, e_3, e_4, \theta, \chi, Y_d) \end{aligned} \tag{26}$$

The controller parameters are selected as:

$$\lambda_1 = \mathbf{M} p(e_1, e_2, e_3, e_4, \theta, \chi, Y_d) - \bar{h}_2 \operatorname{sgn}(\sigma_2) \tag{27}$$

where  $\bar{h}_2 \geq |d_1(t)|$ . Again, the conventional Lyapunov function is  $V = \frac{1}{2} \sigma_2^2$ . Therefore,

$$\begin{aligned} \dot{V} &= \sigma_2(\dot{\mu}_1 - \mathbf{M} \dot{\mu}_2) = \sigma_2(\lambda_1 + d_1(t) - \mathbf{M} \dot{\mu}_2) \\ &= \sigma_2 \{ \mathbf{M} p(e_1, e_2, e_3, e_4, \theta, \chi, Y_d) - \bar{h}_2 \operatorname{sgn}(\sigma_2) + d_1(t) - \mathbf{M} p(e_1, e_2, e_3, e_4, \theta, \chi, Y_d) \} \\ &= \sigma_2 \{ d_1(t) - \bar{h}_2 \operatorname{sgn}(\sigma_2) \} = \sigma_2 d_1(t) - \bar{h}_2 |\sigma_2| \leq 0 \end{aligned} \tag{28}$$

now by executing the vector  $\mathbf{M}$  which is equal to  $\mathbf{M} = [m_1 \ m_2 \ m_3]$  and let  $\tilde{A}_{22} + \tilde{A}_{21} \mathbf{M}$  to be Hurwitz. Then, the following get.

$$\begin{aligned} \tilde{A}_{22} + \tilde{A}_{21} \mathbf{M} &= \begin{bmatrix} 0 & 0 & 0 \\ 0 & 0 & \varepsilon^{-1} \\ 0 & g & 0 \end{bmatrix} + \begin{bmatrix} 1 \\ \varepsilon^{-1} \\ 0 \end{bmatrix} [m_1 \ m_2 \ m_3] = \begin{bmatrix} 0 & 0 & 0 \\ 0 & 0 & \varepsilon^{-1} \\ 0 & g & 0 \end{bmatrix} + \begin{bmatrix} m_1 & m_2 & m_3 \\ \varepsilon^{-1} m_1 & \varepsilon^{-1} m_2 & \varepsilon^{-1} m_3 \\ 0 & 0 & 0 \end{bmatrix} \\ &= \begin{bmatrix} m_1 & m_2 & m_3 \\ \varepsilon^{-1} m_1 & \varepsilon^{-1} m_2 & \varepsilon^{-1} + \varepsilon^{-1} m_3 \\ 0 & g & 0 \end{bmatrix} \end{aligned} \tag{29}$$

Hence,

$$|sI - (\tilde{A}_{22} + \tilde{A}_{21} \mathbf{M})| = s^3 - (m_1 + \varepsilon^{-1} m_2) s^2 - g(\varepsilon^{-1} + \varepsilon^{-1} m_3) s + g \varepsilon^{-1} m_1 \tag{30}$$

based on the rule of Routh, the following relations are obtained (31).

$$m_1 > 0, m_2 < -\varepsilon m_1, m_3 < -\frac{\varepsilon^{-1}m_2}{m_1 + \varepsilon^{-1}m_2} \tag{31}$$

The SMC control parameters ( $c, M, \text{ and } \bar{h}_i$  where  $i = 1, 2$  ) are selected optimally by using the particle swarm optimization (PSO) algorithm technique [27]. The idea behind the PSO technique is that the best solution can be obtained by simulating the movement of the birds. This technique adopted the particles as a population of the individual which flies over the space of solution finding the optimal result or solution. The particles are moving around the search space and each one of these particles has its position and velocity. Hence the evaluation of particles is based on the closest one to the optimal solution and that can be done according to the function named fitness function [27].

The PSO algorithm depended on two main values. the first one is the previous best value named  $pbest$  which is related to the particular particle. The second value named  $gbest$  is the best compared to all the particles  $pbest$  in the overall swarm. The SMC with four weight parameters is arranged in an array to represent the particles. Then initialized all particles randomly and the updating followed afterwards based on (32)-(35) [28] to obtain the optimal values for the sliding mode controller parameters in all cases that encounter the work of the aircraft.

$$\begin{aligned} \Delta c_j^{i+1} &= \Delta c_j^i + k_1 rand_1(pbest_j^i - c_j^i) + k_2 rand_2(gbest^i - c_j^i) \\ c_j^{i+1} &= \Delta c_j^i + \Delta c_j^{i+1} \end{aligned} \tag{32}$$

$$\begin{aligned} \Delta M_j^{i+1} &= \Delta M_j^i + k_1 rand_1(pbest_j^i - M_j^i) + k_2 rand_2(gbest^i - M_j^i) \\ M_j^{i+1} &= \Delta M_j^i + \Delta M_j^{i+1} \end{aligned} \tag{33}$$

$$\begin{aligned} \Delta \bar{h}_{1j}^{i+1} &= \Delta \bar{h}_{1j}^i + k_1 rand_1(pbest_j^i - \bar{h}_{1j}^i) + k_2 rand_2(gbest^i - \bar{h}_{1j}^i) \\ \bar{h}_{1j}^{i+1} &= \Delta \bar{h}_{1j}^i + \Delta \bar{h}_{1j}^{i+1} \end{aligned} \tag{34}$$

$$\begin{aligned} \Delta \bar{h}_{2j}^{i+1} &= \Delta \bar{h}_{2j}^i + k_1 rand_1(pbest_j^i - \bar{h}_{2j}^i) + k_2 rand_2(gbest^i - \bar{h}_{2j}^i) \\ \bar{h}_{2j}^{i+1} &= \Delta \bar{h}_{2j}^i + \Delta \bar{h}_{2j}^{i+1} \end{aligned} \tag{35}$$

where  $j = 1, 2, 3 \dots N_p$ ,  $N_p$  defines as the number of particles,  $c_j^i, M_j^i, \bar{h}_{1j}^i$  and  $\bar{h}_{2j}^i$  define as the particle weight  $j$  at  $i$  iteration,  $k_1$  and  $k_2$  define the constants acceleration which has a value of 2. The values  $rand_1$  and  $rand_2$  represent the random numbers where used here between 0 and 1,  $pbest^i$  defines as the best previous weight of  $j^{th}$  particle, and  $gbest$  is the best particle among all the particles in the population.

The number of dimensions in PSO is equal to four due to the four main controller parameters of the SMC. The model estimation is based on the criterion of the mean square error function as (36), (37).

$$\begin{aligned} E_1 &= \frac{1}{N_p} \sum_m^{N_p} (e_1(i+1))^m)^2 \\ E_2 &= \frac{1}{N_p} \sum_m^{N_p} (e_2(i+1))^m)^2 \end{aligned} \tag{36}$$

$$\begin{aligned} E_3 &= \frac{1}{N_p} \sum_m^{N_p} (e_3(i+1))^m)^2 \\ E_4 &= \frac{1}{N_p} \sum_m^{N_p} (e_4(i+1))^m)^2 \end{aligned} \tag{37}$$

The values of the mean square error ( $E_1 - E_4$ ) must be less than  $1e^{-5}$  to satisfy the optimal tuning. Table 1 presents the parameter values adopted for the solution of the PSO of the current study.

Table 1. PSO parameters

Parameter	Value
$k_1$	1.3
$k_2$	1.3
No. of particles	4
Population size	100
No. of iteration	66

**4. SIMULATION RESULTS AND DISCUSSIONS**

In this section, the analytical derivation of the system given in (3) and the proposed SMC that was derived in (7), (20), and (27) are verified by using the MATLAB platform. The first step is that the main parameters of SMC are selected by try and error procedure. The second step is that the main SMC parameters are tuned optimally based on the swarm optimization technique available in MATLAB options. The following optimal parameters are selected.

$$M = [5 \quad -14 \quad -6], \quad c = 50, \quad \bar{h}_i = \begin{bmatrix} 5 \\ 10 \end{bmatrix} \text{ where } i = 1,2$$

The coefficient of coupling  $\varepsilon$  is taken in the current study as 0.5 where this value produces a non-minimum phase system of VTOL aircraft that is strong [29]. The trajectory of the desired output is assumed as  $x_d = R\sin(\omega t)$ ,  $y_d = R\sin(\omega t)$ , where R is the amplitude and  $\omega$  is the frequency of the desired input. These values, R and  $\omega$ , are taken from 0.1 to 0.2 and 1 to 1.2 respectively to simulate a case of obstacle avoidance [29]. The initial conditions are selected as  $x(0) = [0.5 \ 0.5 \ 0.5 \ -0.05 \ 1 \ 0.5]^T$ .

To represent the present robustness of the proposed controller, the state tracker and generator are assumed as  $\xi_1 = 0.5 \sin t$  and  $\xi_2 = 0.5 \cos t$  and performed the simulation with these values. Notice that  $\xi_1$  and  $\xi_2$  are inertial parameters, which are not important to know their values practically [6]. Figure 2 illustrates the block diagrams of the proposed controller scheme in MATLAB Simulink.

Figures 3-5 show the output tracking simulation results. Figure 3 presents the tracking trajectory of the positioning and the velocity of direction x to the proposed desired trajectory. It is evident that the time required to have zero error is around 2.8 s. Figure 4 presents the tracking trajectory of the positioning and the velocity of direction y to the proposed desired trajectory. The time required to have zero error is the same as that for x-direction. Figure 5 shows the tracking trajectory of the angular positioning and the angular velocity to zero, which is the proposed reference trajectory. It is obvious that the time required to have zero error of the angular positioning and the angular velocity is around 2.4s and 2s respectively.

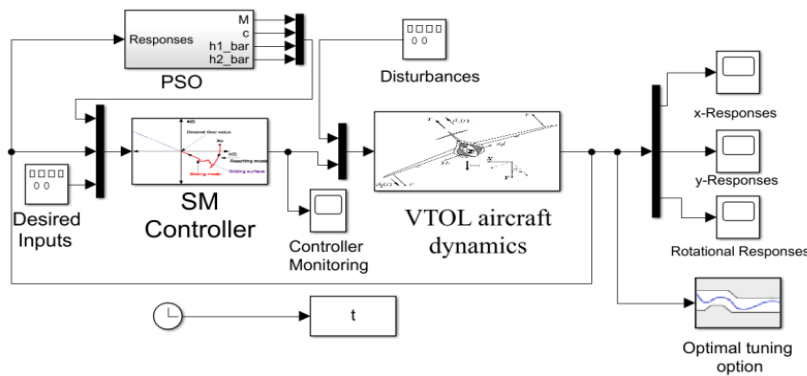


Figure 2. Simulink representation of proposed optimal SMC of VTOL system

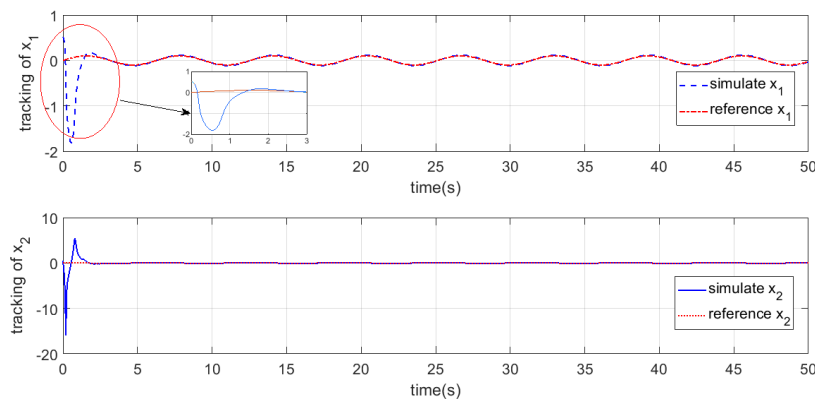


Figure 3. The positioning and velocity responses in x-direction versus the desired responses



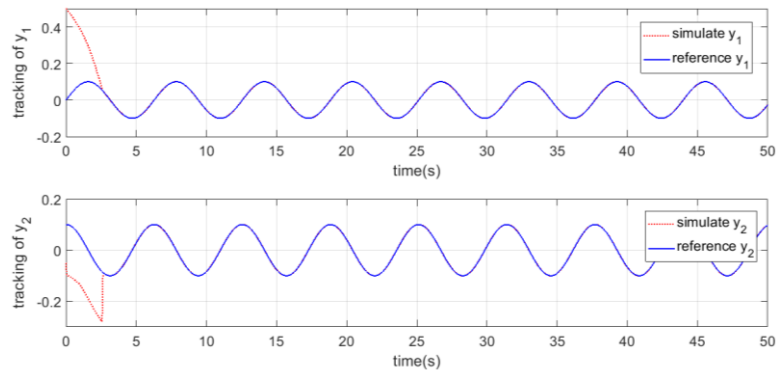


Figure 4. The positioning and velocity responses in the y-direction versus the desired responses

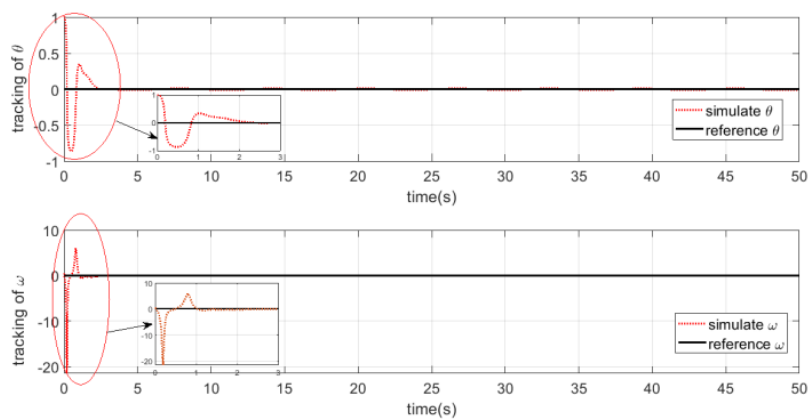


Figure 5. The roll angle versus the zero responses

To monitor the stability of the closed-loop feedback nonlinear optimal SMC for the VTOL system, Figure 6 presents the phase-plane plot for concentrating upon the chattering influence which is discarded due to these causes. The signum function utilized the Sigmoid function,  $sgn(\sigma_i) = c \tanh(\sigma_i)$ , in this study and the control parameters values are calculated by adopting the Particle Swarm optimization algorithm. Figure 7 shows the behaviour of the sliding variable (surface). It is evident that the effect of chattering is highly eliminated at the fast-switching surface. This is due to the use of the signum function which leads to reducing the amplitude of the output function then the responses of VTOL approached the desired responses at the inverted position. It can be noticed that the control inputs,  $u_1$  and  $u_2$ , presented in Figure 8 are rather aggressive behaviours that take place in relatively short periods as well as they are bound. In addition, the selected controller and the controller behaviour are presented in Figures 9 and 10 respectively.

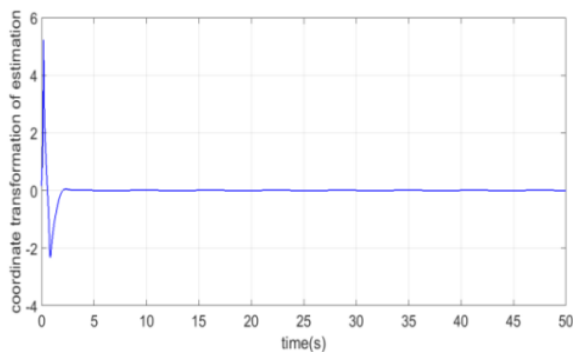


Figure 6. The phase plane response

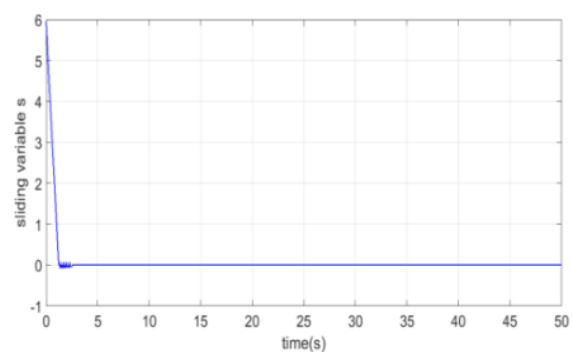


Figure 7. The sliding variable behaviour

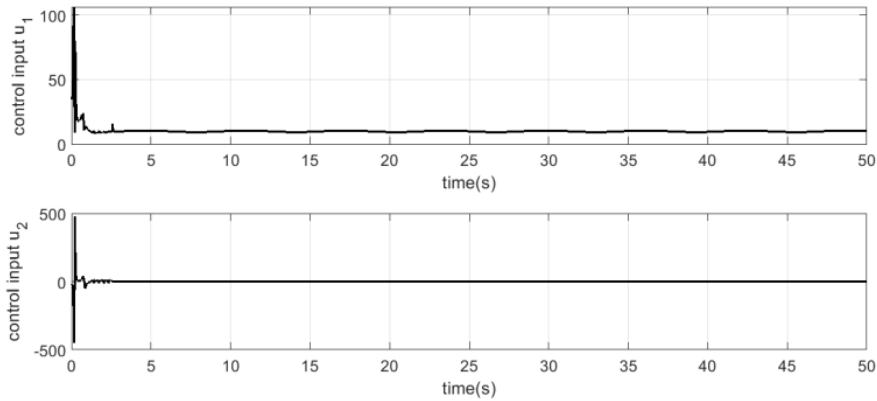


Figure 8. The actuation inputs controls

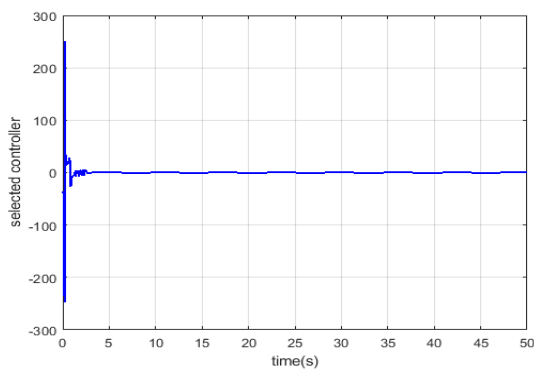


Figure 9. The selected controller behaviour

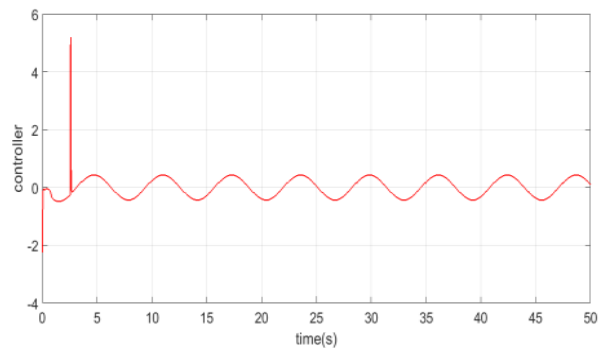


Figure 10. The controller behaviour

For validation purposes, the essential results of this study were compared to some of the literature. Despite the different techniques and the aim in [29], [30], the responses are compared for both positions and velocities. The results for configuration tracking and velocities are shown in Figure 11 according to [30] while the result of roll angle variation is illustrated in Figure 12 according to [29]. By comparing these results with results presented in Figures 3-5, it is evident that the time required for steady-state is improved by 74% and 71% for configuration and velocities respectively according to [30]. In addition, the comparison of roll angle response is 81% less in Figure 3 compared to the results of [29] as shown in Figure 12. These improvement rates show the effectiveness of the proposed controller in this study.

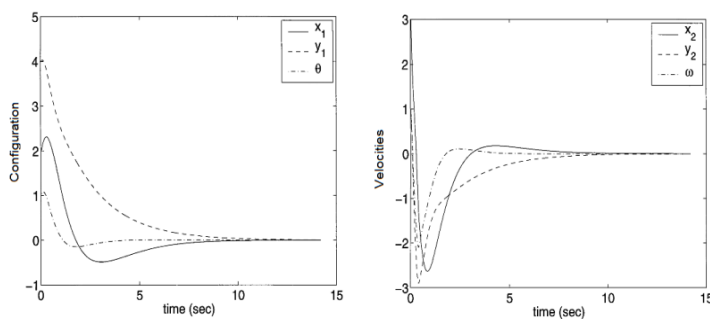


Figure 11. The actual configuration responses versus the desired responses [30]

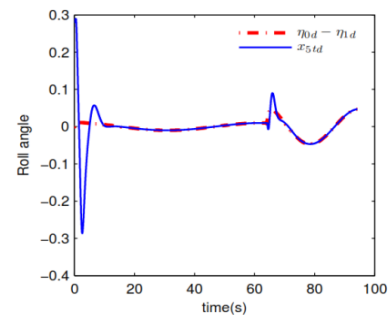


Figure 12. The actual roll angle response versus the desired response [29]

## 5. CONCLUSION

In this study, the dynamics of VTO are analyzed based on Newton's law. The SMC is proposed to track the desired trajectory. The SMC uses a proposed sigmoid function to eliminate the chattering effect. Also, the controller is tuned optimally by using the PSO algorithm technique. In the designed optimal SMC, not only the tracking trajectory is obtained but also the stability is guaranteed based on Lyapunov and Routh's theories. The MATLAB Simulink is used to execute the proposed controller. The results show the significant output responses for all main parameters assumed. The error goes to zero in a very significant period not reaching 3 sec. The validation results showed an improvement average rate reaching about 72% and 84% for reduction into zero steady-state responses according respectively. Not only have these significant responses improved but also stability is achieved when the disturbances are available. Also, the chattering which is an SMC disadvantage property is highly eliminated as well.





## REFERENCES

- [1] A. Intwala and Y. Parikh, "A review on vertical take off and landing (vtol) vehicles," *International Journal of Innovative Research in Advanced Engineering (IJIRAE)*, vol. 2, pp. 187-191, 2015.
- [2] A. Tayebi and S. McGilvray, "Attitude stabilization of a four-rotor aerial robot," in *2004 43rd IEEE Conference on Decision and Control (CDC)(IEEE Cat. No. 04CH37601)*, pp. 1216-1221, 2004, doi: 10.1109/CDC.2004.1430207.
- [3] H. Voos, "Nonlinear state-dependent Riccati equation control of a quadrotor UAV," in *2006 IEEE Conference on Computer Aided Control System Design, 2006 IEEE International Conference on Control Applications, 2006 IEEE International Symposium on Intelligent Control*, 2006, pp. 2547-2552, doi: 10.1109/CACSD-CCA-ISIC.2006.4777039.
- [4] M. Sato and K. Muraoka, "Flight controller design and demonstration of quad-tilt-wing unmanned aerial vehicle," *Journal of guidance, control, and dynamics*, vol. 38, pp. 1071-1082, 2015, doi: 10.2514/1.G000263.
- [5] J. Hauser, S. Sastry, and G. Meyer, "Nonlinear control design for slightly non-minimum phase systems: Application to V/STOL aircraft," *Automatica*, vol. 28, pp. 665-679, 1992, doi: 10.1016/0005-1098(92)90029-F.
- [6] P. Martin, S. Devasia, and B. Paden, "A different look at output tracking: Control of a VTOL aircraft," *Automatica*, vol. 32, pp. 101-107, 1996, doi: 10.1109/CDC.1994.411460.
- [7] F. Lin, W. Zhang, and R. D. Brandt, "Robust hovering control of a PVTOL aircraft," *IEEE Transactions on Control Systems Technology*, vol. 7, pp. 343-351, 1999, doi: 10.1109/87.761054.
- [8] L. Marconi, A. Isidori, and A. Serrani, "Autonomous vertical landing on an oscillating platform: an internal-model based approach," *Automatica*, vol. 38, pp. 21-32, 2002, doi:10.1016/S0005-1098(01)00184-4.
- [9] K. D. Do, Z.-P. Jiang, and J. Pan, "On global tracking control of a VTOL aircraft without velocity measurements," *IEEE Transactions on Automatic Control*, vol. 48, pp. 2212-2217, 2003, doi: 10.1109/TAC.2003.820148.
- [10] A. Ailon, "Simple tracking controllers for autonomous VTOL aircraft with bounded inputs," *IEEE Transactions on Automatic Control*, vol. 55, pp. 737-743, 2010, doi: 10.1109/TAC.2010.2040493.
- [11] C. Hançer, K. Oner, E. Sirimoglu, E. Çetinsoy, and M. Unel, "Robust hovering control of a quad tilt-wing UAV," in *IECON 2010-36th Annual Conference on IEEE Industrial Electronics Society*, pp. 1615-1620, 2010, doi: 10.1109/IECON.2010.5675441.
- [12] S. Bouabdallah, A. Noth, and R. Siegwart, "PID vs LQ control techniques applied to an indoor micro quadrotor," in *2004 IEEE/RSJ International Conference on Intelligent Robots and Systems (IROS)(IEEE Cat. No. 04CH37566)*, pp. 2451-2456, 2004, doi: 10.1109/IROS.2004.1389776.
- [13] B. Erginer and E. Altug, "Modeling and PD control of a quadrotor VTOL vehicle," in *2007 IEEE Intelligent Vehicles Symposium*, pp. 894-899, 2007, doi: 10.1109/IVS.2007.4290230.
- [14] Z. Kong and Q. Lu, "Mathematical modeling and modal switching control of a novel tiltrotor UAV," *Journal of Robotics*, vol. 2018, pp. 1-12, 2018, doi: 10.1155/2018/8641731.
- [15] K. T. Öner *et al.*, "Mathematical modeling and vertical flight control of a tilt-wing UAV," *Turkish Journal of Electrical Engineering & Computer Sciences*, vol. 20, pp. 149-157, 2012, doi: 10.3906/elk-1007-624.
- [16] S. L. Waslander, G. M. Hoffmann, J. S. Jang, and C. J. Tomlin, "Multi-agent quadrotor testbed control design: Integral sliding mode vs. reinforcement learning," in *2005 IEEE/RSJ International Conference on Intelligent Robots and Systems*, 2005, pp. 3712-3717, doi: 10.1109/IROS.2005.1545025.
- [17] R. Czyba and G. Kronhof, "Motion equations and longitudinal control of a convertible VTOL aircraft," in *2020 7th International Conference on Control, Decision and Information Technologies (CoDIT)*, 2020, pp. 1029-1034, doi: 10.1109/CoDIT49905.2020.9263980.
- [18] D. N. Cardoso, S. Esteban, and G. V. Raffo, "A new robust adaptive mixing control for trajectory tracking with improved forward flight of a tilt-rotor UAV," *ISA Transactions*, vol. 110, pp. 86-104, 2021, doi:10.1016/j.isatra.2020.10.040.
- [19] Q. Yao, "Robust constrained trajectory tracking control for a PVTOL aircraft subject to external disturbances," *International Journal of Systems Science*, vol. 52, pp. 2617-2629, 2021, doi: 10.1080/00207721.2021.1892862.
- [20] Y.-W. Choe and G.-S. Byun, "Robust controller design for a VTOL plane," in *Systems modelling and optimization*, ed: Routledge, pp. 459-467, 2022.
- [21] M. Mousaei, J. Geng, A. Keipour, D. Bai, and S. Scherer, "Design, modeling and control for a Tilt-rotor VTOL UAV in the presence of actuator failure," *arXiv preprint arXiv:2205.05533*, 2022, doi: 10.48550/ARXIV.2205.05533.
- [22] X. Wang, J. Liu, and K.-Y. Cai, "Tracking control for VTOL aircraft with disabled IMUs," *International Journal of Systems Science*, vol. 41, pp. 1231-1239, 2010, doi: 10.1080/00207720903244048.
- [23] S. Su and Y. Lin, "Output tracking control for a velocity-sensorless VTOL aircraft with measurement delays," *International Journal of Systems Science*, vol. 46, pp. 885-895, 2015, doi: 10.1080/00207721.2013.801091.
- [24] A. S. Al-Araji, "An adaptive swing-up sliding mode controller design for a real inverted pendulum system based on Culture-Bees algorithm," *European Journal of Control*, vol. 45, pp. 45-56, 2019, doi: 10.1016/j.ejcon.2018.12.001.
- [25] Z. Song, J. Hou, H. Hofmann, J. Li, and M. Ouyang, "Sliding-mode and Lyapunov function-based control for battery/supercapacitor hybrid energy storage system used in electric vehicles," *Energy*, vol. 122, pp. 601-612, 2017, doi:10.1016/j.energy.2017.01.098.





- [26] S. Kava, "Dynamics and control of a quadrotor aircraft," *Dynamics and Control*, vol. 5, p. 8, 2016.
- [27] D. Wang, D. Tan, and L. Liu, "Particle swarm optimization algorithm: an overview," *Soft computing*, vol. 22, pp. 387-408, 2018, doi: 10.1007/s00500-016-2474-6.
- [28] A. Ghoul, K. Kara, M. Benrabah, and M. L. Hadjili, "Optimized nonlinear sliding mode control of a continuum robot manipulator," *Journal of Control, Automation and Electrical Systems*, pp. 1-9, 2022.
- [29] S. Su and Y. Lin, "Approximate trajectory tracking control of a velocity-sensorless VTOL aircraft with measurement delays," in *2011 50th IEEE Conference on Decision and Control and European Control Conference*, 2011, pp. 2499-2504, doi: 10.1109/CDC.2011.6160355.
- [30] R. Olfati-Saber, "Global configuration stabilization for the VTOL aircraft with strong input coupling," *IEEE Transactions on Automatic Control*, vol. 47, pp. 1949-1952, 2002, doi: 10.1109/TAC.2002.804457.

## BIOGRAPHIES OF AUTHORS







**Wajdi Sadik About**     is currently a lecturer at the Prosthetics and Orthotics engineering department/college of engineering/Al-Nahrain university as an associated professor. He obtained a BEng degree in Mechanical Engineering from the University of Al-Nahrain, Iraq in 1992. He then worked in the aircraft maintenance workshops before joining the Foundation of Technical Education in 2003 as a member of the academic staff. He then received the MSc degree in Mechanical Control Design from the University of Technology, Iraq in 2005. He had done his PhD at UKM (National University of Malaysia) in 2014. His field of specialization is in control and mechatronic systems. His current research interests include the control of hybrid and switched dynamic systems and mechatronic systems for automotive and robotic applications. He can be contacted at email: wajdisadik@gmail.com.







**Hayder S. Abd Al-Amir**     is currently a lecturer at the Power Mechanics Department, Institute of Technology-Baghdad, Middle Technical University as an associated professor. He obtained a BEng degree in Mechanical Engineering from the University of Technology, Iraq in 1994. He then received the MSc degree in Applied Mechanics from the Jordan University of Science and Technology, Jordan in 1997. He then worked in the Foundation of Technical Education in 2006 as a member of the academic staff. He had done his Ph.D. at the University of Technology in 2012. His field of specialization is in control, mechatronic systems and vibrations. He can be contacted at email: dr.hayder\_sabah108@mtu.edu.iq.



**Aseel A. Alhamdany**     is currently a lecturer at the Electromechanical Engineering department/ University of Technology as an associated professor. She obtained a BEng degree in Mechanical Engineering from the University of Al-Nahrain, Iraq in 1995. She is a member of the academic staff since 2001. She received her MSc degree in the Electromechanical Engineering department at the University of Technology, Iraq in 2001. She had done her Ph.D at the University of Technology in 2011. Her field of specialization is in Modeling mechanical properties. Her current research interests include applied mechanics. She can be contacted at email: Aseel.A.Abdulrazak@uotechnology.edu.iq.



**Fahad M. Kadhim**     was born in Najaf, Iraq. He obtained a BEng degree in Mechanical Engineering from the Al-Kufa University-Najaf, Iraq in 2011. He then received the MSc degree in Mechanical Engineering from Al-Nahrain University-Baghdad, Iraq in 2013. He had done his PhD at Al-Nahrain University in 2020. He is currently a lecturer at the Prosthetics and Orthotics engineering department/college of engineering/Al-Nahrain university as a lecturer. His field of specialization is in the dynamics and analysis of smart prostheses. His current research interests include applied mechanics. He can be contacted at email: Fahadmohanad@gmail.com.